Material Forming - ESAFORM 2023 Materials Research Forum LLC
Materials Research Proceedings 28 (2023) 331-338 https://doi.org/10.21741/9781644902479-36

Investigation of the compaction behavior of uni- and bidirectional non-crimp fabrics

SCHÄFER Bastian[1,a *], ZHENG Ruochen[2], BOISSE Philippe[2] and KÄRGER Luise[1]

[1]Karlsruhe Institute of Technology (KIT), Institute of Vehicle System Technology (FAST), Karlsruhe, Germany

[2]Université de Lyon, LaMCoS CNRS, INSA-Lyon, F-69621, France

[a]bastian.schaefer@kit.edu, [b]ruochen.zheng@insa-lyon.fr, [c]philippe.boisse@nsa-lyon.fr, [d]luise.karger@kit.edu

Keywords: Fabrics/Textiles, Experimental Characterization, UD-NCF, Biax-NCF

Abstract. The through-thickness compaction behavior of engineering textiles significantly influences the resulting component properties during liquid composite molding processes (LCM). It determines the final fiber volume content and thus the necessary press force, the permeability as well as the final mechanical properties. In the present work, the behavior of a uni- and bidirectional carbon fiber non-crimp fabric (UD- & Biax-NCF) with the same fiber type and areal density of fibers in the respective main reinforcement directions is tested in a punch-to-plate setup. Thereby, the influence of the relative fiber orientation at the interfaces of a layup as well as the number of plies is investigated. A combined influence of roving nesting and superposition of stitching patterns is observed. This results in a common influence of decreasing resistance to compaction for higher numbers of layers, while the relative orientation of the interfaces in a layup is only significant for the Biax-NCF.

Introduction

Non-crimp fabrics (NCFs) have straight fibers compared to woven fabrics with undulated fibers and therefore provide a higher lightweight potential. The resulting component properties during liquid composite molding processes are significantly influenced by the through-thickness compaction behavior. It determines the final fiber volume content (fvc) and thus the necessary press force, the permeability as well as the resulting mechanical properties [1]. The compaction behavior of woven fabrics as well as biaxial NCFs (Biax-NCF) has been investigated more extensively [2-8], compared to unidirectional NCFs (UD-NCF) [9-11].

A typically measured thickness or fvc vs pressure diagram for engineering textiles has two distinct regions: the first region is dominated by a low compression resistance due to the low bending stiffness of crimped fibers and closing of initial gaps between the fibers; in the second region the fibers come into contact with each other and the resistance to compression is more dominated by an increasing number of high Hertzian contact forces [12]. The compaction behavior is largely determined by the architecture of the textile, the type of fiber and the areal density [4, 5, 10]. Textiles with a higher areal density tend to have a smaller resistance to compaction because they have more yarns in a roving and usually a more rounded shape of fiber bundles [4, 7, 13] Additional factors influencing the compaction of multi-ply stacks are the number of layers and layup sequence [7]. Increasing the number of plies in a layup reduces the resistance to compaction, due to rovings of different layers sliding into gaps at the inhomogeneous interfaces. This effect is called nesting and usually more pronounced for woven fabrics compared to NCFs [14]. For NCFs, the compaction behavior is also influenced by the superposition of the stitching patterns and tension in the stitching during production [7, 10, 14].

In a recent benchmark by Yong et al. [8] two glass-fiber fabrics (woven and Biax-NCF) were investigated at over 20 institutes in dry and wet conditions in order to investigate the conformity of compaction test results. Thereby, no distinct influence could be attributed to the size of the specimen, shape of the testing device or weight determination method. However, three main sources for variability were identified: thickness measurement method, machine compliance and specimen saturation in wet compression tests. However, a correction of the machine compliance as described by Sousa et al. [15] led to a good agreement between different institutions.

The compaction behavior of textiles is strongly dependent on the individual properties of the fabric and care must be taken when conducting the experiments to obtain compliant results. In this work, the behavior of a uni- and bidirectional carbon fiber NCF with the same fiber type and areal density of fibers in the respective main reinforcement directions is tested, based on the principles for the measuring method outlined in [15]. Thereby, the influence of the relative fiber orientation at the interfaces of a layup as well as the number of plies is investigated.

Experimental Procedure

Materials.

In this study, a unidirectional (UD300) and bidirectional (MD600) non-crimp fabric both without binder are used. The fabrics are manufactured by Zoltek and produced from the same PX35-50K continuous carbon (CF) fiber heavy tows. Both fabrics are stitched together with a 76 dtex PES yarn in a Tricot pattern. The UD-NCF consists of a single layer of aligned CF tows with thin glass fibers (GF) on the back for improved handleability and the MD-NCF of two layers in a 0°/90° orientation. Both fabrics have a similar number of CFs with about 300 g/m^2 in their respective main reinforcing directions. The most relevant characteristics of the NCFs used in this study are listed in Table 1.

Table 1. Characteristics of the investigated NCFs.

	Stitching length	*Tow width*		*Areal density*			
		0°	*90°*	*Total*	*0°*	*90°*	*stitching*
Unit	[mm]	[mm]	[mm]	[g/m^2]	[g/m^2]	[g/m^2]	[g/m^2]
UD300	3.6	5.0	-	328.86	309.86	9.7 (GF)	9.3
MD600	2.6	5.0	2.5	602.24	301.53	292.52	8.19

Punch-to-plate compaction tests.

The compaction behavior is investigated with a simple punch-to-plate setup mounted on a universal testing machine with a 50 kN load cell, cf. Fig. 1 a). Undeformed stacks of two, four, six or eight plies with a size of 200 x 200 mm^2 are compacted with a 150 x 160 mm^2 punch at a constant speed of 1 mm/min. Each measurement is repeated four times with a new stack of material for each test. Additionally, three different layups for each material are investigated with relative orientations of $\Delta\Theta = 0°, 45°\ or\ 90°$ between the CFs at the interfaces of each ply in a stack, cf. Fig. 1 b). In the UD-NCF layups, the front side (f) of the fabric with a zigzag pattern is facing up for each ply. This is the same for the Biax-NCF in layups with a relative interface orientation of $\Delta\Theta = 45°$ or 90°, while every second ply is flipped over with its back side (b) facing up for $\Delta\Theta = 0°$. The fabrics were stacked randomly to represent the typical case of an automated stacking process.

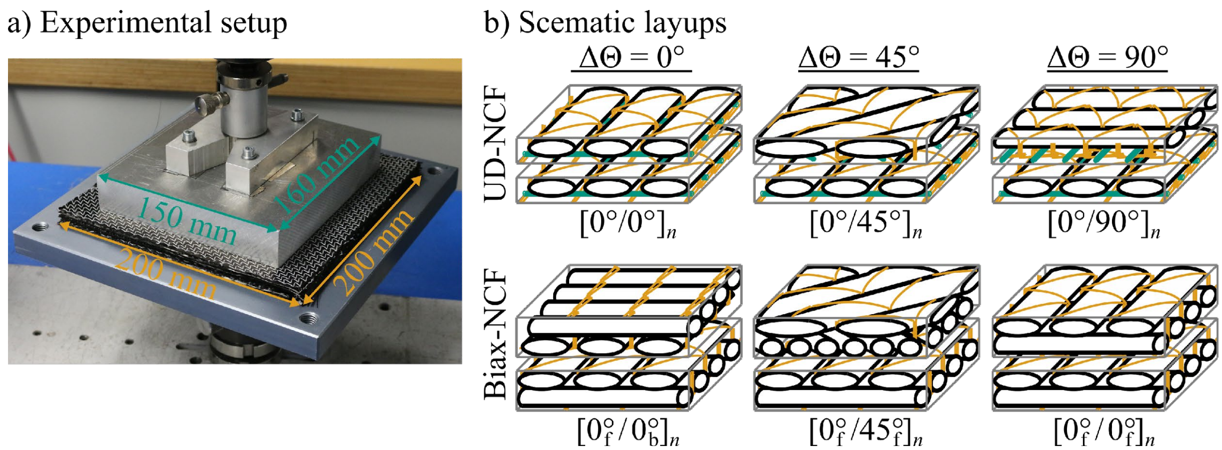

Fig. 1. a) Experimental punch-to-plate compaction test setup; b) Schematic lay-ups of the investigated combinations for different relative fibre orientations at the interfaces with the PES stitching of the NCFs in orange and the GF in green.

The fabric stacks of n_L-plies are compacted to a remaining thickness t_{rem} equivalent to a theoretical fiber volume content Φ of 65 %, cf. Fig. 2 a), according to

$$\Phi = \frac{m_A \cdot n_L}{\rho_{CF} \cdot t_{rem}} = \frac{(m_{total} - m_{stitching} - m_{GF}) \cdot n_L}{\rho_{CF} \cdot t_{rem}}, \quad (1)$$

where $\rho_{CF} = 0.00181\ g/mm^3$ is the density of the utilized CFs and m_A is the areal density of the CFs in the stack, which is approximated by subtracting the weight of the stitching $m_{stitching}$ and GFs m_{GF} from the total measured areal density m_{total}.

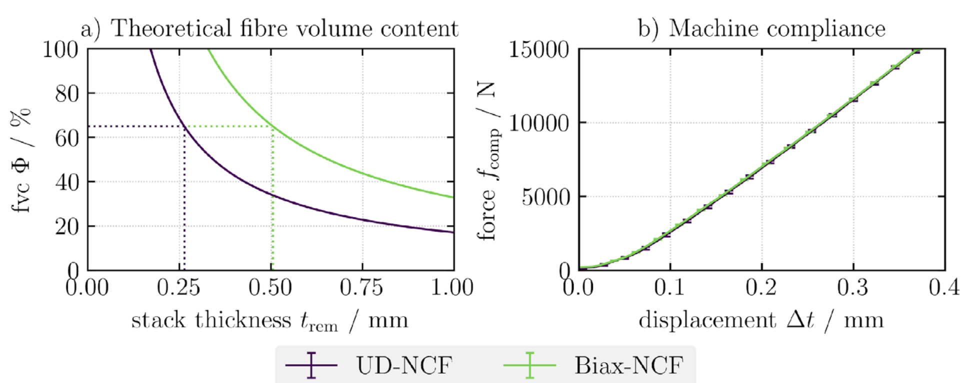

Fig. 2. a) Theoretical fibre volume content for a single layer ($\mathbf{n_L = 1}$) according to Eq. 1; b) Machine compliance curve during the loading stage.

Machine compliance adjustment.

Based on the results of the recent benchmark conducted by Yong et al. [8], machine compliance has a significant influence on the measured thickness during compaction tests. Therefore, the machine compliance was measured based on the method outlined by Sousa et al. [15]. Without a fabric, the top and bottom plates are brought into contact with each other ($\Delta t = 0$) and further pressed together with a prescribed speed of 1 mm/min. The machine force is measured as a function of the cross-head displacement, cf. Fig. 2 b). The results were used to correct the true remaining stack thickness t_{rem} of each trial according to

$$t_{rem} = t_{meas} - \Delta t(f_{comp}), \tag{2}$$

where t_{meas} is the measured thickness according to the cross-head displacement reading and $\Delta t(f_{comp})$ is the thickness correction depending on the compaction force. The slight non-linearity of the curves indicates a small instability in the testing setup caused by non-controlled elements in the testing fixtures used (e.g. un-parallelism of the plates, internal friction, different materials). However, a good agreement is found between the compliance curve measured prior to testing of the UD- and Biax-NCF.

Results and Discussion

Influence of machine compliance.

In order to highlight the importance of adjusting the results for machine compliance, especially for varying numbers of layers n_L, Fig. 3 shows the results of the UD-NCF for the $[0°/0°]_n$-layups with ($[0°/0°]_n$) and without ($[0°/0°]_n^{\mathrm{raw}}$) machine compliance adjustment. Especially for high fiber volume contents, Φ is linear in n_L but very sensitive to small changes in the individual ply thickness, cf. Eq. 1. Since the compaction forces for all configurations are of the same order of magnitude, the thickness correction Δt results in larger deviations for the final fvc for fewer layers. This results in a deviation of $\Delta\Phi = 8 - 15\%$ from the targeted final fvc of $\Phi^{\mathrm{target}} = 65\%$. The maximum forces reduce due to the averaging over the smallest common resulting stack thickness t_{rem} among all trials after adjustment according to Eq. 2. Most importantly, however, the position of the curves changes in relation to each other. While an increase in the resistance to compaction is observed for the raw data, a decrease is observed after taking the machine compliance into account.

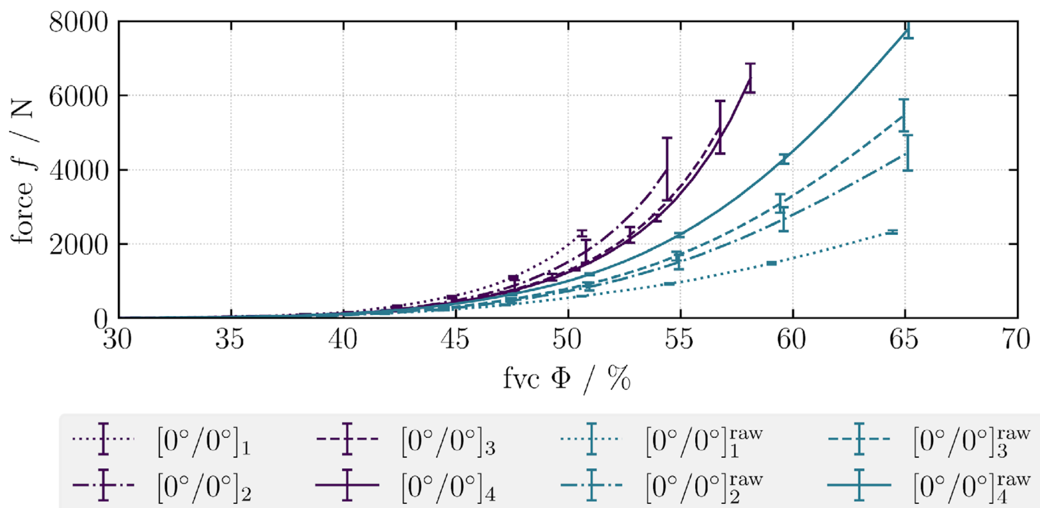

Fig. 3. Influence of the machine compliance adjustment on the results for UD-NCF with a $[\mathbf{0°/0°}]_{\boldsymbol{n}}$-layup.

Influence of the number of layers n_L.

The resulting forces over fiber volume content for different $\Delta\Theta$ are presented in Fig. 4. All compaction curves show the well-known non-linear shape with progressively increasing forces [2]. For Biax-NCF the resistance to compaction decreases for an increasing number of layers independent of the layup sequence due to nesting of the layers. This observation is more pronounced for a $\Delta\Theta$ of 0° or 90°. The offset of 45° decreases the area of superimposed stitching seams compared to continuously stacked layups [7]. This also results in a smaller scatter in the experimental results for $\Delta\theta = 45°$. Since the layers were stacked randomly, it is possible for stitching patterns for a $\Delta\Theta$ of 0° or 90° to coincide between the layers causing an increased resistance to compaction for some of the trials as shown by Korkiakoski et al. [10]. The decrease in resistance to compaction seems to diminish as the number of layers increase, indicating a threshold for even higher n_L. In literature, this threshold is reached at about 10-15 layers for many textiles [2, 3, 6].

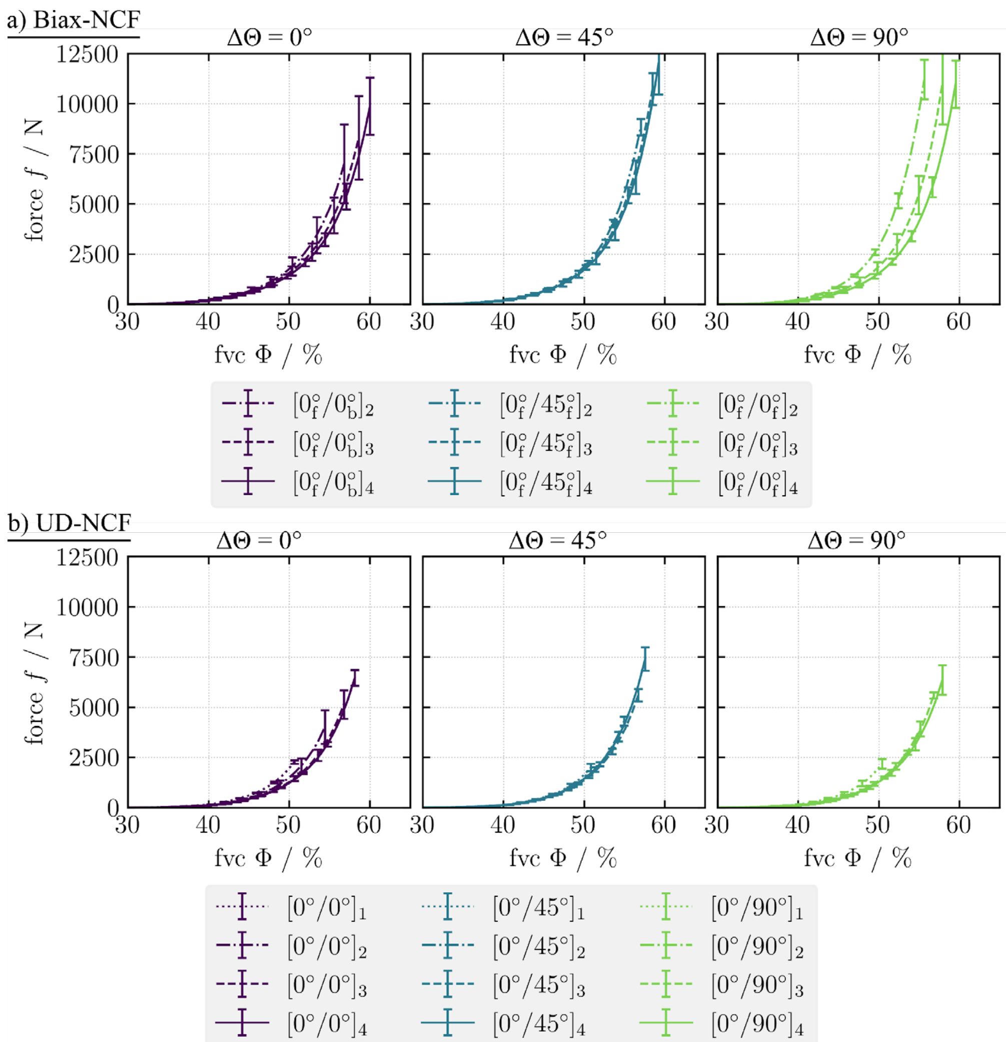

Fig. 4. Compaction test results for different relative interface orientations Θ | a) Biax-NCF; b) UD-NCF.

A similar trend is observed for the UD-NCF, but mainly for an increase of n_L from two to four, cf. Fig. 4 b). A further increase of the number of layers only slightly affects the compaction response with strongly overlapping experimental scatter. Presumably, the GF on the back of the UD-NCF prevent such a strong nesting effect as for Biax-NCF. For $\Delta\Theta = 45°$ the results for $n_L = 8$ is even lower compared to $n_L = 6$ and all curves in general are closer to each other just like for the Biax-NCF. This further indicates a noticeable influence of the superimposed stitching. The threshold for the influence of n_L for the UD-NCF seems to be nearly reached for 8 layers, indicated by a very small decrease in the compaction resistance for more than six layers.

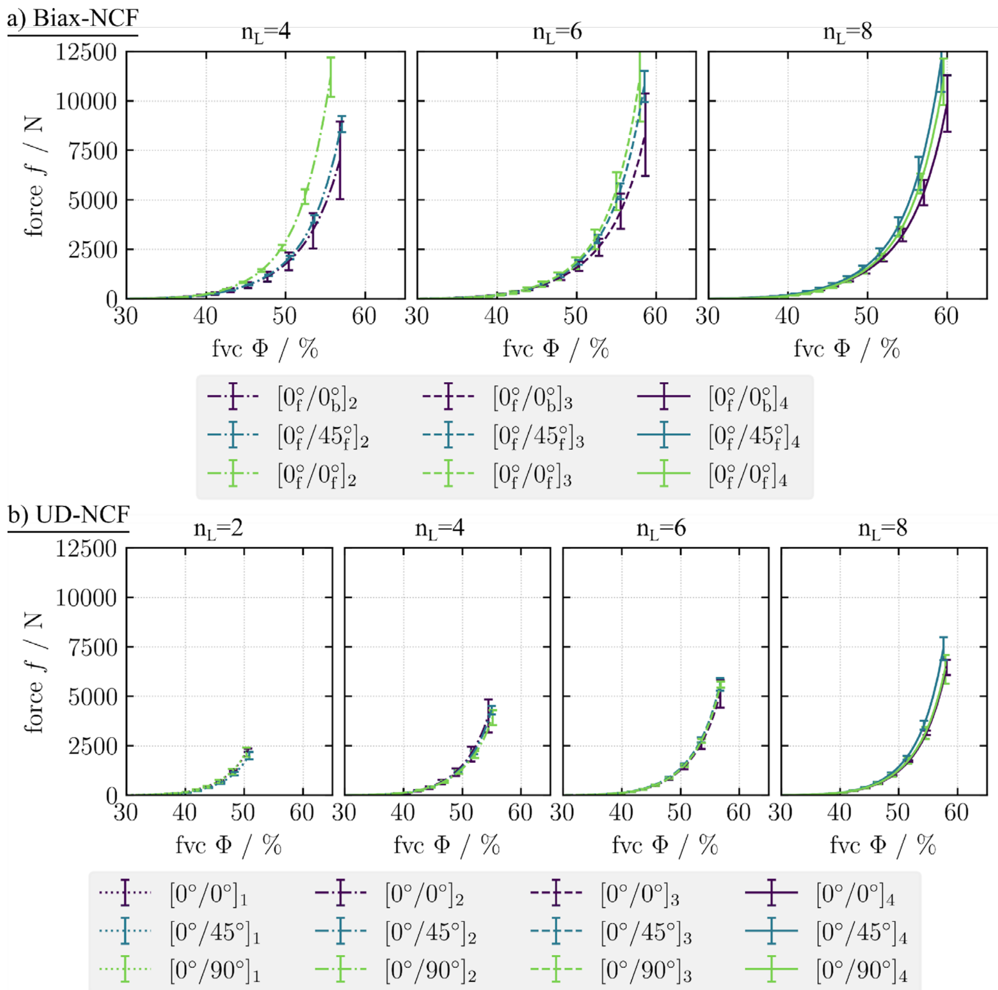

Fig. 5. Compaction test results for different number of layers $\mathbf{n_L}$ | *a) Biax-NCF; b) UD-NCF.*

Influence of the relative interface orientation $\Delta\Theta$.

To make it easier to assess the influence of the relative interface orientations, the results are shown again in Fig. 5 depending on the number of layers n_{L}. For Biax-NCF the $[0^\circ_{\mathrm{f}}/0^\circ_{\mathrm{b}}]_n$-layup requires the smallest compaction force to achieve a targeted fvc independent of n_{L}, cf. Fig. 5 a). This reinforces the assumption that the influence of the number of layers is caused by a combination of nesting of rovings as well as the influence of superimposed stitching patterns. For the $[0^\circ_{\mathrm{f}}/0^\circ_{\mathrm{f}}]_n$-layups, mainly superposition of stitching causes a decreasing resistance to compaction for larger stacks, while for the $[0^\circ_{\mathrm{f}}/0^\circ_{\mathrm{b}}]_n$-layups the effect is amplified by a stronger possibility for nesting of the rovings. In contrast, the compaction behavior of UD-NCF is barely influenced by the relative layer orientation and very similar for the respective number of layers, cf. Fig. 5 b).

Summary

In this work, a study on the compaction behavior of UD- and Biax-NCF for different layup-types and relative fiber orientations at the interfaces is presented. First, the relevance of considering the machine compliance was emphasized, especially in order to study the behavior for different numbers of layers. Comparing the UD- and Biax-NCF to each other, some similarities can be observed. With an increasing number of layers, the resistance to compaction for both materials decreases independent of relative interface orientation. This effect is weakest for $\Delta\Theta = 45^\circ$, indicating a combined influence of roving nesting and superposition of the stitching patterns. The stiffness decrease is smaller for the UD-NCF, which is presumably due to the glass fibers preventing pronounced nesting. For both fabrics, the influence of n_{L} is diminishing, indicating a threshold for these effects. However, more experiments with even more layers are necessary for both materials to identify the exact threshold. An influence of the relative interface orientation is only distinctly observed for Biax-NCF. Turning over every second layer in a $[0^{\circ}_{\mathrm{f}}/0^{\circ}_{\mathrm{b}}]_n$-layup reduces the required forces for a targeted fvc, which can be used to reduce required pressing forces [16].

The results of this study allow a better understanding of the two investigated non-crimp fabrics and could be used to parametrize an analytical or simulation model to design molding processes. Therefore, the compaction behavior for different velocities as well as very high and low numbers of layers should be addressed in further studies.

Acknowledgments
The authors would like to thank the Deutsche Forschungsgemeinschaft (DFG, German Research Foundation) and the French National Research Agency (ANR) for funding the collaborative project "Composite forming simulation for non-crimp fabrics based on generalized continuum approaches" (project number 431354059), which the presented work is carried out for. The work is also part of the Young Investigator Group (YIG) "Tailored Composite Materials for Lightweight Vehicles", generously funded by the Vector Stiftung.

References
[1] C.T. Poppe, C. Krauß, F. Albrecht, L. Kärger, A 3D process simulation model for wet compression moulding, Compos. Part A: Appl. Sci. Manuf. 50 (2021) 106379. https://doi.org/10.1016/j.compositesa.2021.106379
[2] F. Robitaille, R. Gauvin, Compaction of textile reinforcements for composites manufacturing. I: Review of experimental results, Polym. Compos. 19 (1998) 198-216. https://doi.org/10.1002/pc.10091
[3] B. Chen, E.J. Lang, T.-W. Chou, Experimental and theoretical studies of fabric compaction behavior in resin transfer molding, Mater. Sci. Eng. A317 (2001) 188-196. https://doi.org/10.1016/S0921-5093(01)01175-3
[4] S.V. Lomov, M. Barburski, T. Stoilova, I. Verpoest, R. Akkerman, R. Loendersloot, Ten Thije, R. H. W., Carbon composites based on multiaxial multiply stitched preforms. Part 3: Biaxial tension, picture frame and compression tests of the preforms, Compos. Part A: Appl. Sci. Manuf. 36 (2005) 1188-1206. https://doi.org/10.1016/j.compositesa.2005.01.015
[5] J. Yang, J. Xiao, J. Zeng, D. Jiang, C. Peng, Compaction Behavior and Part Thickness Variation in Vacuum Infusion Molding Process, Appl. Compos. Mater. 19 (2012) 443-458. https://doi.org/10.1007/s10443-011-9217-8
[6] L. Li, Y. Zhao, J. Yang, J. Zhang, Y. Duan, An experimental investigation of compaction behavior of carbon non-crimp fabrics for liquid composite molding, J. Mater. Sci. 50 (2015) 2960-2972. https://doi.org/10.1007/s10853-015-8860-0
[7] T. Grieser, P. Mitschang, Investigation of the compaction behavior of carbon fiber NCF for continuous preforming processes, Polym. Compos. 38 (2017) 2609-2625. https://doi.org/10.1002/pc.23854
[8] A.X.H. Yong, A. Aktas, D. May, A. Endruweit, S.V. Lomov, S. Advani, P. Hubert, S.G. Abaimov, D. Abliz, I. Akhatov, M.A. Ali, S. Allaoui, T. Allen, D.C. Berg, S. Bickerton, B. Caglar, P. Causse, A. Chiminelli, S. Comas-Cardona, M. Danzi, J. Dittmann, C. Dransfeld, P. Ermanni, E. Fauster, A. George, J. Gillibert, Q. Govignon, R. Graupner, V. Grishaev, A. Guilloux, M.A. Kabachi, A. Keller, K. Kind, D. Large, M. Laspalas, O.V. Lebedev, M. Lizaranzu, A.C. Long, C. López, K. Masania, V. Michaud, P. Middendorf, P. Mitschang, S. van Oosterom, R. Schubnel, N.

Sharp, P. Sousa, F. Trochu, R. Umer, J. Valette, J.H. Wang, Experimental characterisation of textile compaction response: A benchmark exercise, Compos. Part A: Appl. Sci. Manuf. 142 (2020) 106243. https://doi.org/10.1016/j.compositesa.2020.106243
[9] A. Hammami, B.R. Gebart, Analysis of the vacuum infusion molding process, Polym. Compos. 21 (2000) 28-40. https://doi.org/10.1002/pc.10162
[10] S. Korkiakoski, M. Haavisto, M. Rostami Barouei, O. Saarela, Experimental compaction characterization of unidirectional stitched non-crimp fabrics in the vacuum infusion process, Polym. Compos. 37 (2016) 2692-2704. https://doi.org/10.1002/pc.23464
[11] D. Droste, L. Krishnappa, S. Bornemann, J.-H. Ohlendorf, M.G. Vargas Gleason, A.S. Herrmann, W. Lang, Investigation of the compaction behaviour of a quasi-unidirectional non-crimp fabric during the vacuum infusion process, J. Compos. Mater. 56 (2022) 2509-2524. https://doi.org/10.1177/00219983221092011
[12] P. Boisse, R. Akkerman, P. Carlone, L. Kärger, S.V. Lomov, J.A. Sherwood, Advances in composite forming through 25 years of ESAFORM, Int. J. Mater. Form. 15 (2022) 99. https://doi.org/10.1007/s12289-022-01682-8
[13] J. Yang, J. Xiao, J. Zeng, D. Jiang, C. Peng, Compaction Behavior and Part Thickness Variation in Vacuum Infusion Molding Process, Appl. Compos. Mater. 19 (2012) 443-458. https://doi.org/10.1007/s10443-011-9217-8
[14] S.V. Lomov, I. Verpoest, T. Peeters, D. Roose, M. Zako, Nesting in textile laminates: geometrical modelling of the laminate, Compos. Sci. Technol. 63 (2003) 993-1007. https://doi.org/10.1016/S0266-3538(02)00318-4
[15] P. Sousa, S.V. Lomov, J. Ivens, Methodology of dry and wet compressibility measurement, Compos. Part A: Appl. Sci. Manuf. 128 (2020) 105672. https://doi.org/10.1016/j.compositesa.2019.105672
[16] F. Behnisch, V. Lichtner, F. Henning, P. Rosenberg, Development of a Reactive Polyurethane Foam System for the Direct Sandwich Composite Molding (D-SCM) Process, J. Compos. Sci. 5 (2021) 104. https://doi.org/10.3390/jcs5040104